

Increased Sylvian fissure angle as early sonographic sign of malformation of cortical development

R. K. POOH¹, M. MACHIDA¹, T. NAKAMURA¹, K. UENISHI¹, H. CHIYO¹, K. ITOH², J. YOSHIMATSU³, H. UEDA⁴, K. OGO⁴, P. CHAEMSAITHONG⁵  and L. C. POON⁵ 

¹CRIFM Clinical Research Institute of Fetal Medicine Pooh Maternity Clinic, Osaka, Japan; ²Department of Pathology and Applied Neurobiology, Graduate School of Medical Science, Kyoto Prefectural University of Medicine, Kyoto, Japan; ³Department of Obstetrics and Gynecology, National Cerebral and Cardiovascular Center, Osaka, Japan; ⁴Department of Pathology, National Cerebral and Cardiovascular Center, Osaka, Japan; ⁵Department of Obstetrics and Gynaecology, Prince of Wales Hospital, The Chinese University of Hong Kong, Shatin, Hong Kong SAR

KEYWORDS: 3D transvaginal ultrasound; malformations of cortical development; neuronal migration disorder; neurosonography; Sylvian fissure angle

ABSTRACT

Objective To evaluate Sylvian fissure development by assessing Sylvian fissure angles in fetuses with malformation of cortical development (MCD).

Methods This was a retrospective study of 22 fetuses with MCD. Cases with a stored three-dimensional (3D) brain volume acquired at 18 + 0 to 30 + 6 weeks of gestation at an ultrasound-based research clinic between January 2010 and December 2017 were identified through a database. Of the 22 fetuses, seven had an extracranial abnormality, such as cardiac, renal, gastrointestinal and/or digital anomalies, and five had a minor abnormality such as micrognathia, low-set ears and/or single umbilical artery. To confirm the final clinical diagnosis of brain abnormality, postmortem histological findings or prenatal or postnatal magnetic resonance images were used. For measurement of Sylvian fissure angle, an anterior coronal plane of the fetal brain on transvaginal 3D volume multiplanar imaging was visualized as a single image from the three orthogonal views. The right and left Sylvian fissure angles were measured between a horizontal reference line (0°) and a line drawn along the upper side of the respective Sylvian fissure. The Sylvian fissure angle on both sides was plotted on the graphs of the reference ranges for gestational age in weeks.

Results In 21 (95.5%; 95% CI, 86.8–100.0%) of 22 fetuses with MCD, the Sylvian fissure angle on one or both sides was larger than the 90th percentile of the normal reference. There was one case with apparent focal MCD in the parietal lobe, but the Sylvian fissure angles

were normal. A case with apparent unilateral cortical dysplasia and one with apparent unilateral schizencephaly had conspicuous discrepancies between the left and right Sylvian fissure angles. Abnormal genetic test results were obtained in six cases, including four cases with a mutation in a single gene.

Conclusions This study has shown that the Sylvian fissures, as defined by the Sylvian fissure angle, have delayed development in most MCD cases prior to the diagnosis of the condition. The Sylvian fissure angle may potentially be a strong indicator for the subsequent development of cortical malformation, before the time point at which the gyri and sulci become obvious on the fetal brain surface. Further research is required to validate these findings. © 2018 The Authors. *Ultrasound in Obstetrics & Gynecology* published by John Wiley & Sons Ltd on behalf of the International Society of *Ultrasound in Obstetrics and Gynecology*.

INTRODUCTION

Malformations of cortical development (MCD) include a wide range of developmental disorders during the formation of the cerebral cortex and they are one of the most common causes of neurodevelopmental delay and epilepsy^{1,2}. Barkovich *et al.*¹ classified MCD according to recent advances relating to cortical development in the fields of embryology and genetics. Neuronal migration from the first trimester creates a cortical structure consisting of six layers of different nerve cells with distinct morphology and function, and disorders of this process

Correspondence to: Dr R. K. Pooh, CRIFM Clinical Research Institute of Fetal Medicine PMC, 1-24, Uehommachi 7, Tennoji, Osaka 43-0001, Japan (e-mail: rkpooh@me.com or pooh27ritsuko@fetal-medicine-pooh.com)

Accepted: 19 October 2018

are associated with MCD. The consequences of neuronal migration and cerebral cortex development appear as gyri and sulci in late pregnancy. Migration may be impaired in a number of ways, including disorders of mechanical motor and cytoskeletal dynamics of cells, and/or molecular signals that initiate movement, which are essential to guide cell migration and inform their final position³.

Clinically, early detection of MCD is one of the challenges in the field of fetal neuroimaging. During the embryonic stage of brain development, Sylvian fissures appear as shallow depressions on the bilateral surface of the hemispheres following formation of primary fissures that include the interhemispheric, transverse and hippocampal fissures. The Sylvian fissures change markedly in appearance from shallow depressions to deep sulci during the second and third trimesters of pregnancy. It is challenging to determine the exact anatomical landmarks for the same section to guide evaluation of the Sylvian fissures because the fetal brain changes in appearance according to gestational age. In our institute, we have established a strict protocol for orientation of the fetal brain for neuro-assessment and determined several key landmarks for evaluating the fetal brain, including the Sylvian fissures. Figure 1 shows the changing appearance of the Sylvian fissures in the same section between 18 and 30 weeks of gestation. Furthermore, we have established recently a measurable marker for evaluation of the development of the Sylvian fissures, namely the Sylvian fissure angle, and developed normal reference ranges for

the left and right Sylvian fissure angles in a precise anterior coronal section by the determination of key landmarks in three-dimensional (3D) orthogonal planes⁴. The aim of this study was to evaluate Sylvian fissure development by assessing the Sylvian fissure angles in fetuses with MCD.

METHODS

This was a retrospective study utilizing stored 3D volumes of second- and third-trimester fetal brains. The ultrasound examinations used in this study were performed at 18 + 0 to 30 + 6 weeks of gestation at the Clinical Research Institute of Fetal Medicine (CRIFM), Osaka, Japan, between January 2010 and December 2017. The Viewpal (GE Healthcare Ultrasound, Milwaukee, WI, USA) database was used to identify all fetuses with cortical maldevelopment detected on fetal transvaginal neuroimaging and Sylvian fissures of all cases were analyzed retrospectively at CRIFM and Chinese University of Hong Kong. To confirm the final clinical diagnoses of brain abnormality, postmortem histological findings or prenatal or postnatal magnetic resonance imaging was used. Fetuses strongly suspected of having brain abnormality were followed up routinely with serial transvaginal neurosonography. All brain volume acquisitions were performed by the same examiner (R.K.P.). This study was approved by the respective Institutional Review Boards; CRIFM Ref. No. CRI-IRB-008, CRI-IRB-010 and Joint Chinese University

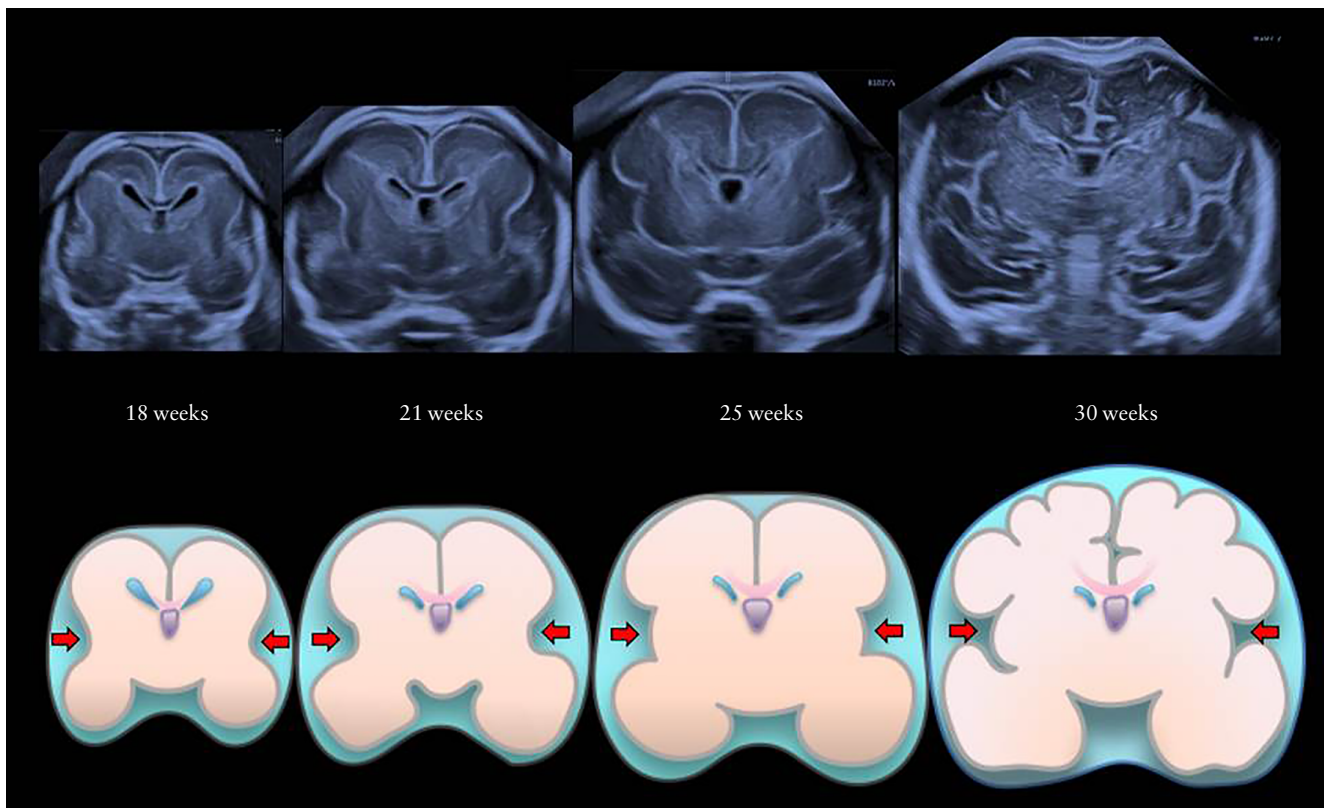


Figure 1 Ultrasound images in anterior coronal section and corresponding schematic diagrams, showing change in appearance of normal Sylvian fissures (arrows) between 18 and 30 weeks of gestation.

of Hong Kong–New Territories East Cluster Clinical Research Ethics Committee, Ref. No. CRE-2017.173.

The ultrasound machine used in this study was a Voluson E8 or E10 (GE Healthcare Ultrasound) with a 6–12-MHz transvaginal 3D transducer. After fetal growth assessment and evaluation of general morphology and fetal Doppler on transabdominal ultrasound, transvaginal neuroimaging was performed. When the fetus was in a non-cephalic position, we waited for the fetus to turn spontaneously to the cephalic position or induced fetal turnover by gentle abdominal manipulation, maternal mobilization and/or maternal rest.

The stored 3D volumes of the selected cases were given to two sonographers (M.M. and T.N.) with extensive experience in ultrasound scanning for the measurement of the Sylvian fissure angles in the anterior coronal view, as described previously⁴. The examiners were unaware of the diagnoses of the cases. The Sylvian fissure angles in each case were then plotted on the reference ranges for gestational age in weeks⁴.

Genetic tests performed included cytogenetic karyotyping, chromosomal microarray (Cytoscan, GeneChip and Chromosome Analysis Suite; Affymetrix Inc., Santa Clara, CA, USA), and/or targeted exome sequencing that included 4813 genes (TruSight™ One Sequencing Panels; Illumina, Inc., San Diego, CA, USA).

RESULTS

Twenty-two fetuses with confirmed MCD were identified and underwent a total of 54 (median, 2.5; range, 1–6) examinations. Of the 22 fetuses, seven had extracranial abnormalities such as cardiac, renal, gastrointestinal and/or digital anomalies, and five had minor findings such as micrognathia, low-set ear and/or single umbilical artery. In all cases, the transvaginal brain assessment was successful. The clinical details of the cases are shown in Table 1, including information of detailed findings on fetal neuroimaging, other complications, gestational age at delivery (in weeks), outcome of pregnancy, postmortem examination findings, final diagnoses and genetic test results. In seven cases, the parents opted for termination of pregnancy before the end of 21 weeks of gestation, which is the legal limit for termination of pregnancy in Japan, and postmortem examination with neuropathological investigations was performed in four of these seven cases. Intrauterine fetal demise occurred at 32 weeks of gestation in one case (Case 22). In the remaining 14 cases, the pregnancy resulted in live birth, of which six were associated with small-for-gestational age at birth. Chromosomal microarray analysis (CMA) was performed in 16 cases when the karyotyping result was normal. Targeted exome sequencing was performed in 11 cases when CMA resulted in no pathogenic copy number variants. In six (31.6%) of the 19 cases in which genetic testing was performed, abnormal genetic results were obtained, including abnormal chromosomal structures (interstitial duplication 6q24.2 → q26/terminal deletion 6q26 → qter and 47,XY,+der(22)t(11;22)(q23.3;q11.2)) and single

gene mutation (paternal 10q uniparental disomy mosaicism with *PTEN* (phosphatase and tensin homolog gene) mutation, *USP9X* (ubiquitin specific peptidase 9 X-linked gene) mutation, *PPP2R1A* (protein phosphatase 2, structural/regulatory subunit A, alpha gene) mutation, and *TMEM67* (transmembrane protein 67 gene) mutation).

Figure 2 shows neurosonographic images of the Sylvian fissures in fetuses with MCD and normal fetuses, according to gestational age, demonstrating delayed Sylvian fissure development in abnormal cases with MCD. The measurements of the fetal right and left Sylvian fissure angles were plotted against the respective reference range (Figure 3). In most cases, the delayed development was symmetrical between the left and right Sylvian fissures. In 21 (95.5%; 95% CI, 86.8–100.0%) of 22 cases with MCD, the Sylvian fissure angle on one or both sides was larger than the 90th percentile of the normal reference. One case (Case 7) had normal Sylvian fissure angle bilaterally but apparent parietal migration disorder. Prenatal images and histological findings of cortical dysplasia with multiple overmigration cell nests and heterotopic cell nests are shown in Figure 4. In two cases (Cases 8 and 14), discrepancy between the right and left Sylvian fissure angles with more than 2.0 SD score was confirmed on a total of three examinations (4.53, 4.20 and 3.52 SD score, respectively). Case 8 was associated with unilateral cortical malformation in the left hemisphere (Figure 5). Histological findings included multiple nodular heterotopia in the left hemisphere. Case 14 had unilateral schizencephaly with cortical matter lined cleft in the left hemisphere (Figure 6).

DISCUSSION

Neuronal cell migration is an important step for cortical formation. Many unique molecular events are involved in moving, organizing and regulating neuronal cells³. The mechanism underlying neuronal migration disorder is far from simple and many complex mechanisms are implicated. MCDs have been classified etiologically by responsible gene mutations and the largest class has been categorized as lissencephaly, which essentially means smooth brain. Due to recent advances relating to cerebral cortical development in the fields of embryology and genetics, MCD is classified into several groups according to genotype rather than phenotype¹ and the classification will evolve with new genetic and embryologic discoveries. However, displaced neurons or heterotopia, which is associated more prevalently with pediatric epilepsy³, can occur in any part of the brain and may arise partially or widely, asymmetrically or symmetrically. Sarnat *et al.*⁵ described that many major brain malformations include a lack of telencephalic flexure, which forms the operculum and finally the Sylvian fissure, or dysplastic Sylvian fissure. Neuronal migration is *per se* cortical development, and therefore many brain malformations may be associated strongly with migration disorder. For example, in some cases with ‘ventriculomegaly’ or ‘agenesis of the corpus callosum’, migration disorder may

Table 1 Characteristics and findings in 22 cases of fetal malformation of cortical development (MCD)

Case	Neuroimaging findings	Extra-CNS findings	GA (wks)	SGA	TOP*	PM	Final diagnosis	Genetic testing
1	MCD, VM due to cerebral hypoplasia, HoCC	—	21	—	Yes	Yes	Multifocal nodular heterotopia, cobblestone type cerebral dysplasia	Karyotype, 46,XY; CMA, normal
2	Cortical maldevelopment	Micrognathia, low-set ears	36	Yes	—	—	MCD	Karyotype, 46,XY; no further genetic exam
3	Cerebral cysts, microcephaly, MCD, cavitation in ganglionic eminence	—	40	—	—	—	Microlissencephaly	Karyotype, 46,XX; CMA, normal; TES, normal
4	MCD, HoCC, VM, asymmetrical irregular ventricular wall, vermian hypoplasia, cysts in bilateral GE	Upper polydactyly (right) unilateral MCDK	37	—	—	—	MCD, polydactyly	Karyotype, 46,XY; CMA, normal; TES, in progress
5	Megalencephaly, severe hypoplastic CC, migration/proliferation disorder	Prominent forehead, low-set ears, micrognathia	21	—	Yes	—	Polygyria, megalencephaly	Karyotype, 46,XY; CMA, paternal 10q UPD mosaicism; TES, <i>PTEN</i> mutation
6	Microcephaly, MCD, cerebellar hypoplasia	Flat face, micrognathia, adducted thumbs	35	Yes	—	—	MCD	Karyotype, 46,XY; CMA, normal; TES, normal
7	Focal cortical maldevelopment in bilateral parietal regions	—	21	—	Yes	Yes	Cobblestone type focal cortical dysplasia at parietal cortices, leptomeningeal heterotopia	Karyotype, 46,XY; CMA, normal
8	MCD of whole left hemisphere	—	21	—	Yes	Yes	Multiple heterotopic nodules, cortical polygyria in left hemisphere	Karyotype, 46,XY; no further genetic exam
9	VM, MCD, cerebellar dysplasia	—	21	—	Yes	Yes	Polymicrogyria and extensive neuroblast heterotopia in cortex, multiple nodular protuberance along the ventricular wall, HoCC, cerebellar hypoplasia	Karyotype, 46,XY; CMA, normal; TES, normal
10	Microcephaly, MCD, cerebellar hypoplasia	HLHS	40	—	—	—	MCD, HLHS, infantile death	Karyotype, 46,XX; CMA, interstitial duplication of 6q24.2 → q26, terminal deletion of 6q26 → qter
11	VM, MCD	—	37	—	—	—	MCD	Karyotype, 46,XX; CMA, normal; TES, normal
12	Lissencephaly, AoCC, multiple calcification in brain and placenta, cerebral dysplasia, MCD, microcephaly	—	41	—	—	—	Microlissencephaly	Karyotype, 46,XX; CMA, normal
13	VM, cerebral hypoplasia, MCD, HoCC	—	39	—	—	—	MCD, VM	Not performed
14	Unilateral schizencephaly, interhemispheric cyst, SP defect	—	39	—	—	—	Unilateral (left) schizencephaly	Not performed
15	MCD, cerebellar hypoplasia	HLHS, cleft lip/palate	39	Yes	—	—	MCD, HLHS, cleft lip/palate	Karyotype, 46,XX; CMA, normal
16	VM, MCD	Duodenal atresia	30	Yes	—	—	MCD, duodenal atresia	Karyotype, 46,XX; CMA, normal; TES, <i>USP9X</i> mutation
17	HoCC, MCD, asymmetrical VM	—	30	Yes	—	—	HoCC, MCD, VM	Not performed
18	Asymmetrical VM, thick hyperechogenic ventricular zone, partial AoCC, hypoplastic cerebra and cerebellum, MCD	Micrognathia, low-set ears, excessive coiling cord	21	—	Yes	—	Mild VM, cerebellar hypoplasia, MCD	Karyotype, 46,XX; CMA, normal; TES, normal

Contd. over.

Table 1 Continued

Case	Neuroimaging findings	Extra-CNS findings	GA (wks)	SGA	TOP*	PM	Final diagnosis	Genetic testing
19	Microcephaly, vermian hypoplasia, abnormal brain cyst, MCD	Placental multiple calcification, small kidneys	40	Yes	—	—	MCD	Karyotype, 47,XY, +der(22)t(11;22)(q23.3;q11.2)
20	VM with cortical maldevelopment, cerebellar hypoplasia	Cleft lip/palate, micrognathia, scoliosis	21	—	Yes	—	VM, MCD, cleft lip/palate, micrognathia, low-set ears	Karyotype, 46,XY; CMA, normal; TES, normal
21	MCD, mild VM, HoCC	SUA	36	—	—	—	HoCC, MCD, VM	Karyotype, 46,XX; CMA, normal; TES, <i>PPP2R1A</i> mutation
22	Vermian defect, molar tooth sign, VM, MCD	Thick cardiac ventricular wall, MCDK, oligohydramnios,	32	—	—	—	Joubert syndrome, IUFD	Karyotype, 46,XX; CMA, normal; TES, <i>TMEM67</i> mutation

*Termination of pregnancy (TOP) < 22 weeks. AoCC, agenesis of the corpus callosum; CC, corpus callosum; CMA, chromosomal microarray analysis; GA, gestational age at delivery; GE, ganglionic eminence; HLHS, hypoplastic left heart syndrome; HoCC, hypogenesis of the corpus callosum; IUFD, intrauterine fetal demise; MCDK, multicystic dysplastic kidney; PM, postmortem examination; *PPP2R1A*, protein phosphatase 2, structural/regulatory subunit A gene, alpha; *PTEN*, phosphatase and tensin homolog gene; SGA, small-for-gestational age (< -1.5 SD); SP, septum pellucidum; SUA; single umbilical artery; TES, targeted exome sequencing; *TMEM67*, transmembrane protein 67 gene; UPD, uniparental disomy; *USP9X*, ubiquitin specific peptidase 9 X-linked gene; VM, ventriculomegaly; wks, weeks.

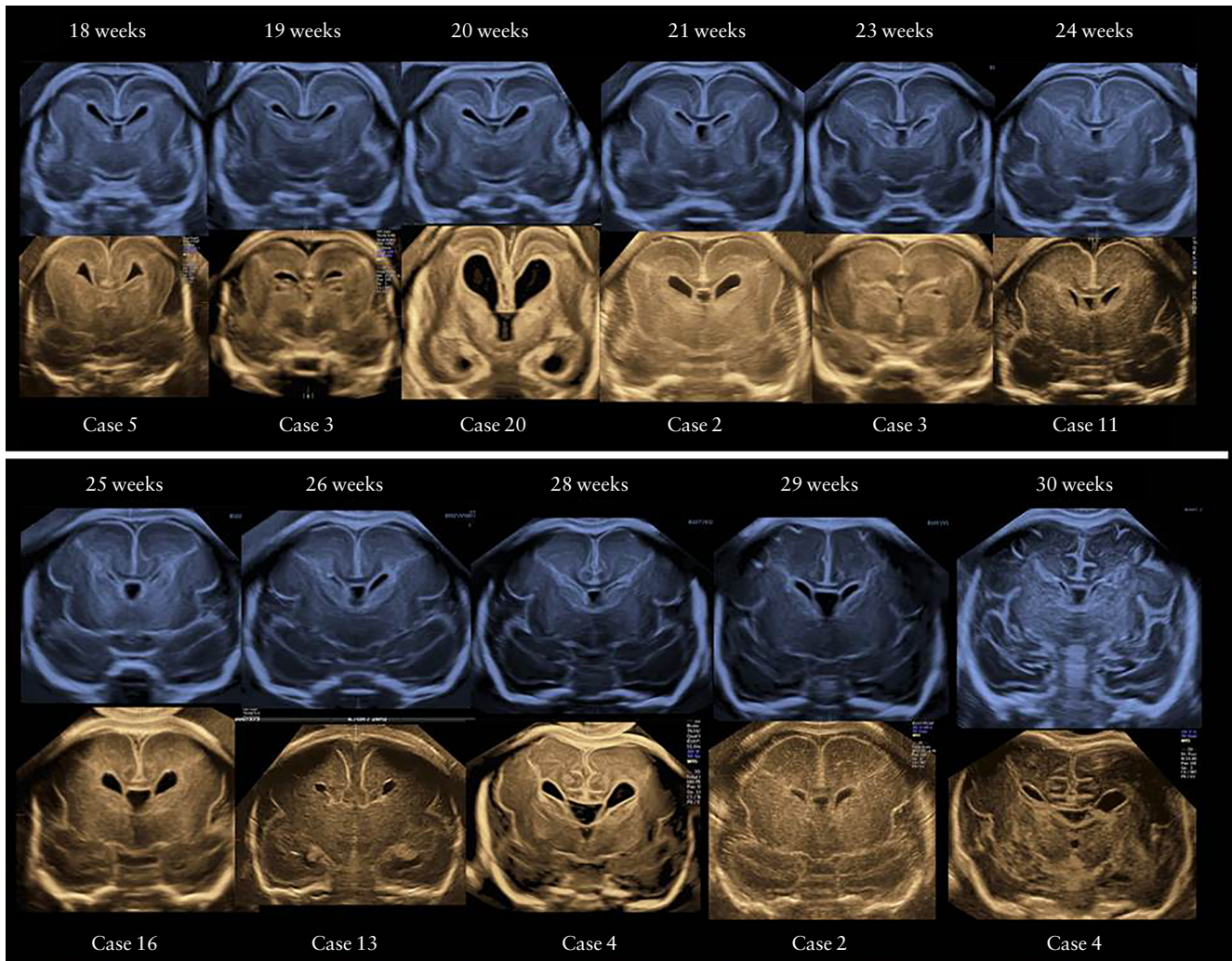


Figure 2 Pairs of ultrasound images of Sylvian fissures in fetuses with malformations of cortical development (lower images) compared with those in normal cases (upper images), according to gestational age.

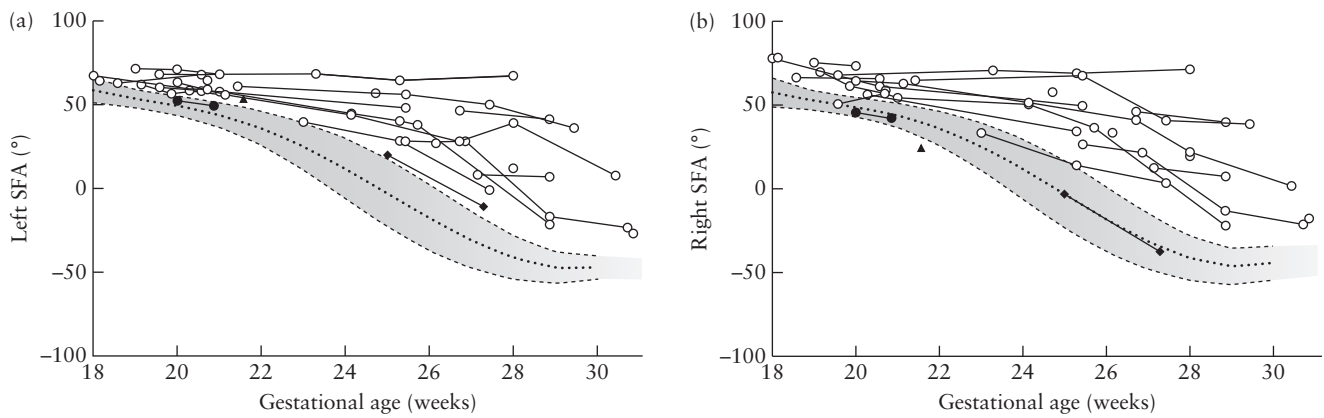


Figure 3 Left (a) and right (b) Sylvian fissure angles (SFA) in 22 fetuses with malformations of cortical development, according to gestational age; 10th, 90th and 50th percentiles of normal reference ranges are shown. Case 7 (●) had normal SFA on both sides, Case 8 (▲) had left > right SFA (SD score = 4.53) and Case 14 (◆) had left > right SFA (SD score = 4.20 and 3.52 at 25 and 27 weeks' gestation, respectively).

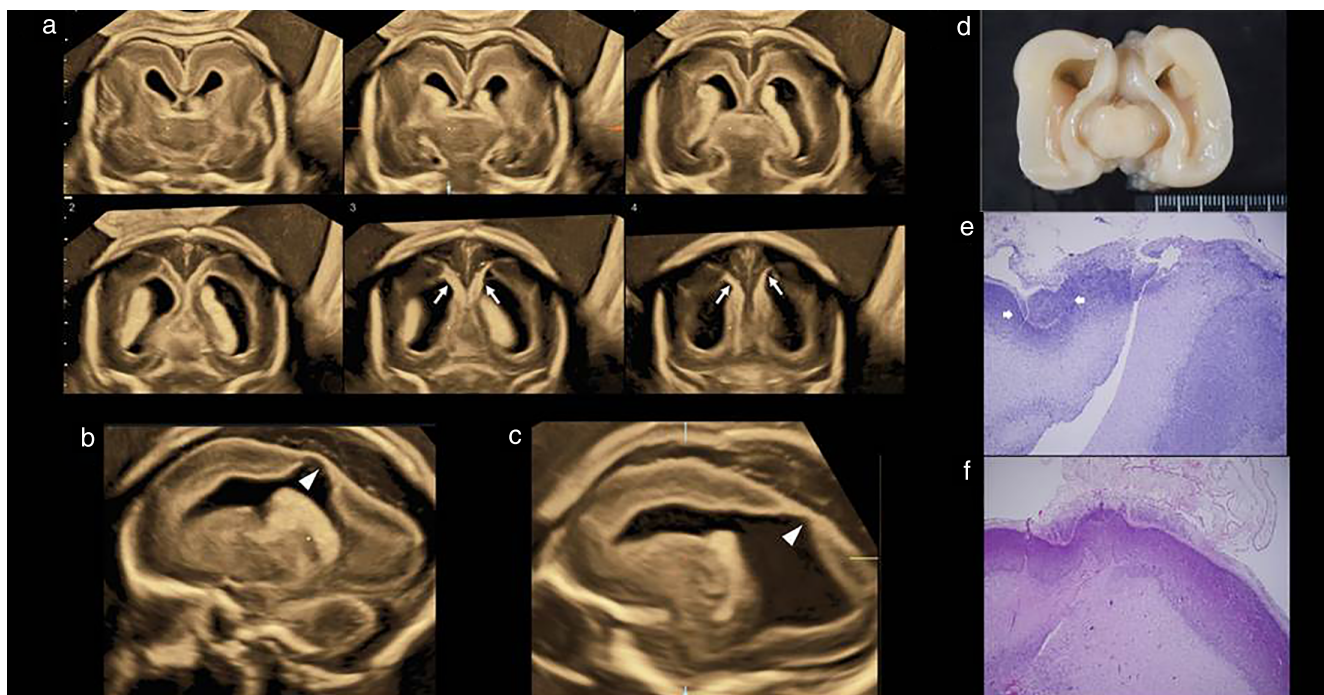


Figure 4 Prenatal ultrasound images and postmortem histological findings in fetus (Case 7) with normal Sylvian fissure angles but focal malformation of cortical development. (a) Tomographic ultrasound images in coronal section; Sylvian fissures appear to be normal but abnormal hyperechoic and thin cerebral tissue (arrows) is seen in middle-to-posterior sections. (b,c) Parasagittal sections showing abnormal lateral ventricular wall with thin cerebral tissue (arrowheads). (d) Macroscopic brain on postmortem examination. (e,f) Histological findings showing cortical dysplasia with multiple overmigration cell nests and heterotopic cell nests.

be latent as the cause of ventriculomegaly or agenesis of the corpus callosum. If this is the case, the prognosis may be worse than expected from the viewpoint of 'isolated ventriculomegaly' or 'isolated agenesis of the corpus callosum'. As described above, early detection of migration disorder or MCD is one of the missions in the field of fetal neuroimaging, in order to achieve accurate diagnoses of fetal brain malformations, appropriate prenatal counseling and proper perinatal management.

Over the past two decades, efforts have been made to visualize cerebral cortical development. In 1997, Montegudo and Timor-Tritsch first described the fetal sulci, gyri and fissures by 2D transvaginal sonography⁶. The

lateral sulcus was visualized from 18 weeks of gestation in a coronal section and from 22 weeks of gestation in a parasagittal section. In 2006, Cohen-Sacher *et al.* published a longitudinal transabdominal/transvaginal study, and reported that the detection rate of the Sylvian fissure was 100% at 18 weeks of gestation⁷. Toi *et al.* first described in 2004 the classification of the Sylvian fissure into smooth (not angular), obtuse angle and acute angle on transabdominal 2D ultrasound⁸. In 2007, Mittal *et al.* used transabdominal 3D multiplanar imaging and attempted to evaluate the Sylvian fissure⁹. Thereafter, several articles have been published on the evaluation of the Sylvian fissure on neuroimaging^{10–16}. In a recent

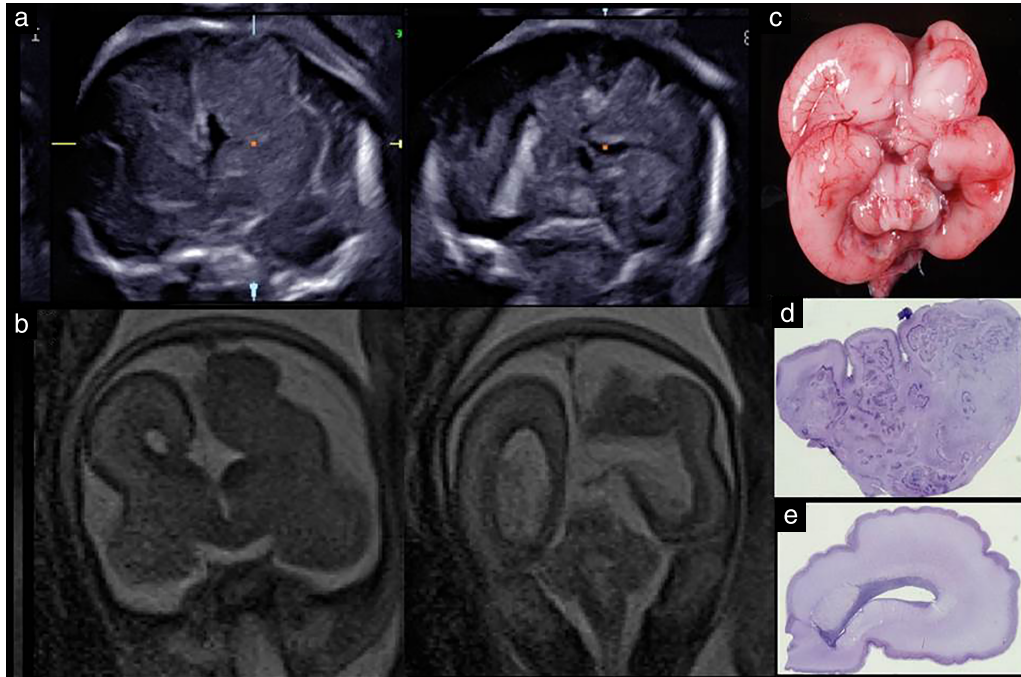


Figure 5 Prenatal images and histological findings in fetus (Case 8) with malformation of cortical development and discrepancy between right and left Sylvian fissure angles. (a) Prenatal ultrasound images in coronal section; abnormal cortical formation is seen in left hemisphere. (b) Fetal magnetic resonance images in coronal section. (c) Macroscopic brain on postmortem examination. (d) Histology of left hemisphere, showing cortical dysplasia with multiple nodular heterotopia. (e) Histology of right hemisphere. Note discrepancy in intracerebral histology between left and right hemispheres.

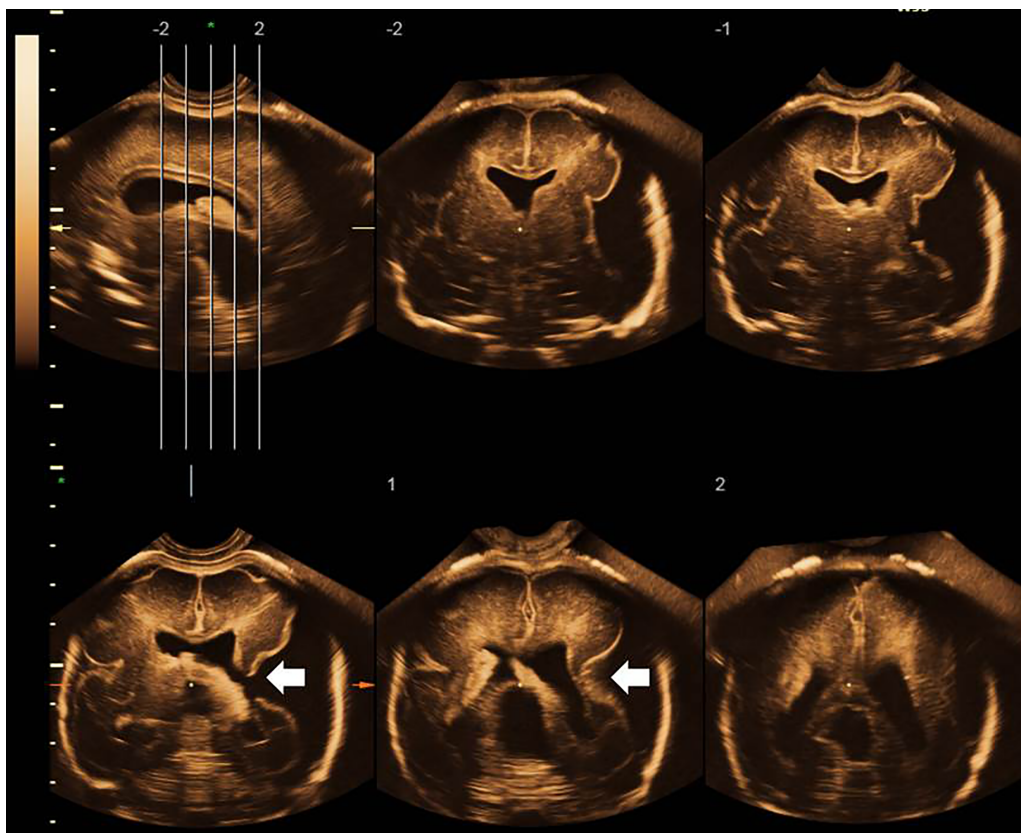


Figure 6 Prenatal ultrasound images in fetus (Case 14) with malformation of cortical development and discrepancy between right and left Sylvian fissure angles at 27 weeks of gestation. Unilateral schizencephaly (arrows) is apparent in left hemisphere.

study by Hahner *et al.* on cortical development on transabdominal/transvaginal neurosonography, a Sylvian fissure grading scheme was described by the use of the axial section¹⁷. As far as we know, there have been no studies describing the precise protocol that would allow visualization of the fetal brain symmetrically.

In our institute, 3D transvaginal brain assessment has been performed for more than a decade and it has aided diagnosis of cortical maldevelopment in several aspects. In particular, we have reported previously that the observations of premature appearance and evolving appearance of the Sylvian fissure are associated with neuronal migration disorder¹⁰. However, we have also encountered difficult cases with very subtle changes in the Sylvian fissure at around 20 weeks of gestation and fully realized the necessity of an objective assessment of the Sylvian fissures. We have established normal reference ranges of the right and left Sylvian fissure angles in the same anterior coronal section by strict determination of the anatomical landmarks in the transvaginal 3D orthogonal planes⁴. In all 22 cases in this study, the fetal brain examinations were performed successfully using transvaginal 3D neuroimaging. Therefore, the stored 3D volumes allowed the application of the manipulation protocol in order to achieve the precise anterior coronal section required for the measurement of the Sylvian fissure angles.

In this study, in 95.5% of the cases of MCD, the Sylvian fissure angle on one or both sides measured between 18 and 30 weeks of gestation was above the 90th percentile of the normal reference. This finding indicates that the Sylvian fissure appears prematurely because of migration disorder and it is suggested that the Sylvian fissure angle may be a strong indicator for early detection of MCD during this period. Two cases had asymmetric measurements between the right and left Sylvian fissure angles due to different migration between the left and right hemispheres. It is therefore necessary to measure both angles and for this the transfontanelle approach is better in comparison with the transabdominal axial approach by which the proximal Sylvian fissure is not well visualized due to acoustic shadowing by the cranial bones. However, the transvaginal approach may potentially be technically more challenging in cases of microcephaly or small fontanelles or when the head is not fully engaged. One case had normal Sylvian fissure angles but had obvious migration disorder. In this case, migration disorder was strongly suspected on the sections of the posterior coronal and parasagittal planes (Figure 4). Considering that cortical maldevelopment may occur in a focal area, it is impossible to detect all MCDs by simply measuring the Sylvian fissure angles in the anterior coronal plane. For comprehensive fetal neuroimaging, evaluation of the whole brain is indicated, using the best technique and equipment available, preferably by the transvaginal approach.

In our series, genetic testing was performed in 19 cases, including chromosomal microarray analysis and 4813 gene-targeted exome sequencing procedures that included congenital cortical maldevelopment-related genes. Six (31.6%) cases had abnormal genetic results, suggesting

that there is a significant association between MCD and genetic abnormalities. Further genetic investigation, such as whole exome or whole genome sequencing, can be considered in cases without pathogenic results on chromosomal microarray analysis or targeted exome sequencing.

The strengths of this study include confirmation of the clinical diagnoses of brain abnormalities by all possible means, complete outcome follow-up, and that all brain volume acquisitions using the transfontanelle approach were performed by the same examiner. The main limitation is the retrospective design of the study. To minimize bias, the stored 3D volumes of the cases were reviewed by two independent sonographers for the measurement of the Sylvian fissure angles and they were unaware of the diagnoses of the cases.

In conclusion, this study has shown that the Sylvian fissures, as defined by the Sylvian fissure angle, have delayed development in most fetuses with MCD prior to the diagnosis of the condition. The Sylvian fissure angle may potentially be a strong indicator for the subsequent development of cortical maldevelopment, before the time point at which the gyri and sulci become obvious on the fetal brain surface. Further research will be required to validate these findings.

REFERENCES

1. Barkovich AJ, Guerrini R, Kuzniecky RI, Jackson GD, Dobyns WB. A developmental and genetic classification for malformations of cortical development: update 2012. *Brain* 2012; 135: 1348–1369.
2. Guerrini R, Dobyns WB. Malformations of cortical development: clinical features and genetic causes. *Lancet Neurol* 2014; 13: 710–726.
3. Ross ME, Walsh CA. Human brain malformations and their lessons for neuronal migration. *Annu Rev Neurosci* 2001; 24: 1041–1070.
4. Poon LC, Sahota D, Chaemsaitong P, Nakamura T, Machida M, Naruse K, Wah IYM, Leung TY, Pooh RK. Transvaginal three-dimensional assessment of Sylvian fissures at 18–30 weeks' gestation. *Ultrasound Obstet Gynecol* 2019; 54: 190–198.
5. Sarnat HB, Flores-Sarnat L. Telencephalic flexure and malformations of the lateral cerebral (Sylvian) fissure. *Pediatr Neurol* 2016; 63: 23–38.
6. Monteagudo A, Timor-Tritsch IE. Development of fetal gyri, sulci and fissures: a transvaginal sonographic study. *Ultrasound Obstet Gynecol* 1997; 9: 222–228.
7. Cohen-Sacher B, Lerman-Sagie T, Lev D, Malinger G. Sonographic developmental milestones of the fetal cerebral cortex: a longitudinal study. *Ultrasound Obstet Gynecol* 2006; 27: 494–502.
8. Toi A, Lister WS, Fong KW. How early are fetal cerebral sulci visible at prenatal ultrasound and what is the normal pattern of early fetal sulcal development? *Ultrasound Obstet Gynecol* 2004; 24: 706–715.
9. Mittal P, Gonçalves LF, Kusanovic JP, Espinoza J, Lee W, Nien JK, Soto E, Romero R. Objective evaluation of sylvian fissure development by multiplanar 3-dimensional ultrasonography. *J Ultrasound Med* 2007; 26: 347–353.
10. Pooh RK. Fetal neuroimaging of neural migration disorder. *Ultrasound Clinics* 2008; 3: 541–552.
11. Guibaud L, Selleret L, Larroche JC, Buenerd A, Alias F, Gaucherand P, Des Portes GV, Pracros JP. Abnormal Sylvian fissure on prenatal cerebral imaging: significance and correlation with neuropathological and postnatal data. *Ultrasound Obstet Gynecol* 2008; 32: 50–60.
12. Lerman-Sagie T, Malinger G. Focus on the fetal Sylvian fissure. *Ultrasound Obstet Gynecol* 2008; 32: 3–4.
13. Quarello E, Stirnemann J, Ville Y, Guibaud L. Assessment of fetal Sylvian fissure operculization between 22 and 32 weeks: a subjective approach. *Ultrasound Obstet Gynecol* 2008; 32: 44–49.
14. Alves CM, Araujo Júnior E, Nardoza LM, Goldman SM, Martinez LH, Martins WP, Oliveira PS, Moron AF. Reference ranges for fetal brain fissure development on 3-dimensional sonography in the multiplanar mode. *J Ultrasound Med* 2013; 32: 269–277.
15. Gindes L, Malach S, Weisz B, Achiron R, Leibovitz Z, Weissmann-Brenner A. Measuring the perimeter and area of the Sylvian fissure in fetal brain during normal pregnancies using 3-dimensional ultrasound. *Prenat Diagn* 2015; 35: 1097–1105.
16. Chen X, Li SL, Luo GY, Norwitz ER, Ouyang SY, Wen HX, Yuan Y, Tian XX, He JM. Ultrasonographic characteristics of cortical sulcus development in the human fetus between 18 and 41 weeks of gestation. *Chin Med J (Engl)* 2017; 130: 920–928.
17. Hahner N, Puerto B, Perez-Cruz M, Policiano C, Monderde E, Crispi F, Gratacos E, Eixarch E. Altered cortical development in fetuses with isolated nonsevere ventriculomegaly assessed by neurosonography. *Prenat Diagn* 2018; 38: 365–375.